ACS OMEGA

Open Access

http://pubs.acs.org/journal/acsodf

Article

Spray Momentum Flux Novel Estimation Procedure through the Fuel Rate of Injection Using Hydrogenated Fuels with Single Hole Nozzle Diesel Injector

Lis Corral-Gómez, Octavio Armas,* José A. Soriano, José-Ignacio Nogueira, and Gabriela Bracho

Cite This: https://doi.org/10.1021/acsomega.3c06917

Read Online

ACCESS | Metrics & More | Article Recommendations

ABSTRACT: Sustainable means of transport require the innovation or development of propulsive systems more respectful of the environment. Despite current criticism, modern compression-ignition engines are efficient alternatives also in light aviation and surveillance drones (such as small helicopters), as means of air transport. Currently, the improvement of the injection, air-fuel mixture formation, and combustion processes using sustainable synthetic fuels, produced from renewable raw materials or by carbon dioxide capture, is a reality. For improving the air-fuel mixture formation inside the combustion chamber, one of the key parameters is knowledge of the spray momentum flux because of its effect on the air entrainement. To measure this parameter is complex. However, the experimental determination of the fuel mass flow rate is a common procedure. The objective of this work is the proposal of a novel but robust methodology for the momentum flux estimation of fuel sprays from measurement of the rate of injection. In this work, single-hole nozzles of 115, 130, and 150 μm in diameter are studied. The implemented methodology is applied to three fuels: a diesel fuel without biodiesel, used as reference, and two sustainable synthetic fuels: a gas to liquid fuel and a hydrotreated vegetable oil. With the fuel injection rates and the simple model proposed, the spray momentum flux is estimated under different operating conditions of a common-rail injection system. The results of the spray momentum flux show a very good precision compared with those experimentally and previously obtained with similar fuels but with multihole nozzle. With the method proposed in this work, an adequate forecast of spray momentum flux is obtained in the case of not having an experimental setup that allows direct measurement of the momentum flux. This study can help investigators for fuel spray modeling with novel and renewable fuels in modern propulsive systems.

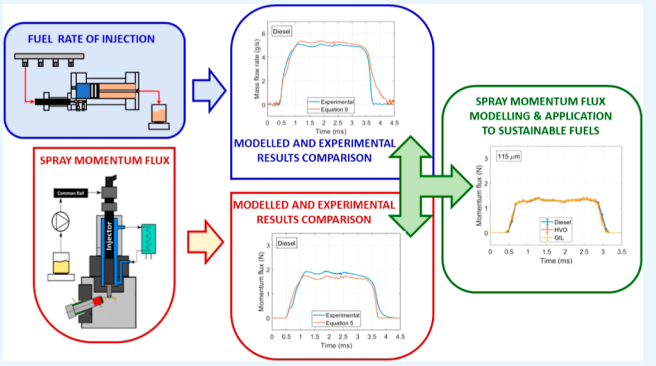

1. INTRODUCTION

Researchers and vehicle manufacturers have focused their attention on keeping the exhaust gas emissions emitted by vehicles as low as possible due to the implementation of increasingly restrictive regulations. On the other hand, governments are becoming considerably concerned about ensuring their energy security due to the rapid decline and limitation of fossil fuel reserves caused by society's high demand for energy, thus also causing an increase in armed conflicts and fuel prices.[1,2]

All of the above has given the use of alternative fuels in vehicles a big boost. Alternative fuels have the capacity to decarbonize the energy generated in internal combustion engines (ICE) because their origin can be partially or totally renewable. In addition, the synthetic nature of these fuels means that they can be adapted and modified to reduce polluting emissions.[3]

Hydrotreated vegetable oil (HVO) is an alternative fuel obtained from the hydrotreatment and isomerization of vegetable oils and animal fats. HVO fuel is a combination of paraffinic hydrocarbons with no aromatic or sulfur content. This leads to a reduction in particulate matter (PM) emitted and a reduction in nitrogen oxides (NO_x) emissions.[4,5] Compared to conventional diesel, HVO fuel has a lower density and a higher cetane number (CN).[6−8] The latter helps to considerably reduce the ignition delay and therefore a lower energy release during premixed combustion. In addition, since the lower heating value (LHV) of HVO fuel and conventional diesel fuel are very similar, it is not necessary to change the amount of fuel excessively to achieve an equivalent energy released.[9]

Gas to liquid (GtL) is a fuel synthesized from natural gas using the Fischer−Tropsch process. GtL fuel does not contain sulfur,

Received: September 11, 2023
Revised: November 18, 2023
Accepted: November 22, 2023

and the amount of aromatic compounds is negligible. This and the lower carbon/hydrogen ratio decrease soot formation. Like HVO fuel, GtL fuel has a higher CN and lower density compared with diesel fuel. These differentiating characteristics benefit the reduction of NO_x emissions.[10−15]

There are some important factors to keep in mind when considering the issue of using alternative fuels in engines. These comprise combustion characteristics, performance, and emissions. These, in turn, depend on factors such as injection pressure, injection start, amount of fuel injected, number of injections, combustion chamber design, and nozzle spray patterns. A good understanding of fuel atomization characteristics is essential to increase combustion efficiency and reduce emissions.[16−20]

There are two experimental procedures for characterizing fuel spray: momentum flux (MF) and rate of injection (RoI). The MF consists of measuring the impact of the fuel on a piezoelectric sensor that is inside a chamber filled with an inert gas.[21,22] This parameter is very important for predicting the blend potential of injection processes to achieve an efficient combustion process with low pollutants formation. Important factors such as spray penetration and cone angle, and air entrainment largely depend on the spray impulse.[23−27] Knowing this parameter, information is obtained about the flow exit velocity and the mass flow rate, thus controlling the air−fuel mixing together with the ambient density.[28−30]

The RoI consists of measuring the pressure variation caused by the injection event by means of a piezoelectric transducer inside a pressurized tube filled with liquid fuel.[31] With the combination of these two measurements, it is possible to determine the hydraulic coefficients of the orifices, discharge coefficient (C_d) and area coefficient (C_a), estimate the flow velocity at the outlet of the injector and evaluate the cavitation that occurs within the injector hole.[32−35]

From fuel injection rates and with the help of the simple model proposed, the spray MF is estimated under different operating conditions for the common-rail injection system used in this work. With the method proposed in this work to obtain the MF from the experimental measurements of mass flow rate, an adequate forecast of this value is obtained in the case of not having an experimental setup that allows the MF. The results from this methodology will help researchers and engine developers in fuel spray modeling with novel and renewable fuels in modern propulsive systems.

In most cases, both facilities are rarely available simultaneously to determine both parameters. Therefore, the objective of this study is to present a methodology to determine the MF based on the measurements of the RoI. Once the method is validated, it is used for characterizing different alternative fuels and nozzle sizes. The work was carried out with three different fuels (HVO, GtL and diesel) and three different nozzles (115, 130, and 150 μm) to determine the robustness of the method for the different fuel properties and the different nozzle outlet sections.

The novelty of this work consists of the statement of a simple model, experimentally validated, for the estimation of the spray MF using renewable synthetic fuels from the experimental determination of a more common parameter: the fuel mass flow rate through the injector. The work is divided into four sections. In Section 2, the materials and methods employed in the study are described. In Section 3, the results obtained are shown and discussed. In Section 4, the conclusions of the work are presented.

2. MATERIALS AND METHODS

This section describes the fuels, test matrix, experimental facility, and nozzle discharge coefficient determination from RoI measures. Later, the procedure for estimating the MF from the RoI data is presented.

2.1. Fuels. Three different fuels were tested for the RoI experiments.

- Conventional diesel fuel without biodiesel fuel and with less than 10 ppm sulfur, supplied by Repsol (Spain).
- HVO fuel supplied by Repsol (Spain).
- GtL fuel from natural gas obtained through a low temperature Fischer−Tropsch process supplied by SASOL (South Africa).

Table 1 shows the main physicochemical properties of the tested fuels.

Table 1. Main Properties of the Fuels Tested

properties	diesel	HVO	GtL
C (% w/w)	86.2	85.7	84.67
H (% w/w)	13.8	14.3	15.31
O (% w/w)	0	0	0
density at 15°C (kg/m^3)	835.8	779.1	773.1
density at 40°C (kg/m^3)[a]	827.6	763.5	756.9
viscosity at 40°C (cSt)	2.96	2.87	2.3
CFPP (°C)	−19	−40	−45
flash point (°C)	61	70	63
CN	54.5	75.5	71
HHV (MJ/kg)	45.97	47.24	46.91
LHV (MJ/kg)	43.18	44.20	43.66
distillation (vol.)			
10% (°C)	206.5	265.2	195
50% (°C)	275.9	278.5	260
90% (°C)	344.9	290.4	338

[a]Calculated with eqs 9−11 of the work done by Armas et al.[36]

2.2. Test Matrix. The experimental conditions used for hydraulic characterization are listed in Table 2. Each fuel was evaluated for two injection pressures, one injection duration and one temperature. These conditions were determined according to the most representative values of the real engine conditions.

Table 2. Test Conditions

parameters	value	units
rail pressure	90, 110	MPa
back pressure	5	MPa
energization time	2	ms
fuel temperature	313	K

The injector used is Bosch with serial number 089909/0445110239, which has a set of single-hole nozzles with a K factor of 3.5 and external diameters of 115, 130, and 150 μm. The injector is controlled by Injectronix CRS-4000 equipment. In this equipment, the set point values of the energization time, injection pressure, and frequency are indicated.

2.3. Experimental Facility Description. For this work, an experimental installation designed to simulate the common-rail injection system of any vehicle, regardless of the engine, was used. The fuel is injected into the EVI-2 measurement equipment, which is filled with the same test fuel, and unlike the combustion chamber of the engine, it is in a nonreactive

https://doi.org/10.1021/acsomega.3c06917
ACS Omega XXXX, XXX, XXX−XXX

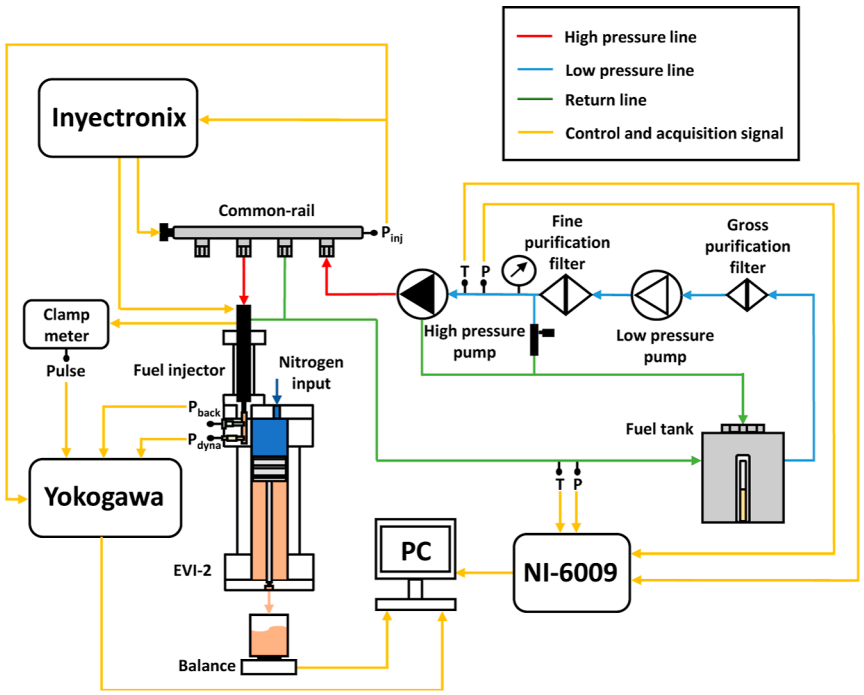

Figure 1. Scheme of the experimental facility.

atmosphere (N_2). Figure 1 shows the scheme of the experimental facility.

The fuel is at rest in the tank of the experimental facility; here, the fuel is conditioned to the set point temperature by means of resistors and an external heat exchanger. The fuel is driven through the circuit with the help of a low-pressure pump to the high pressure pump, which is driven by an electric motor. Before reaching the high pressure pump, the fuel is filtered and purged to remove any particles and air it may contain. The fuel is then pressurized by a high-pressure pump and guided to the common-rail, which contains a pressure regulator that allows the fuel to be maintained at the set injection pressure.

When the fuel is conditioned in temperature and pressure, it is injected into the EVI-2 measurement equipment. The equipment is pressurized by nitrogen to generate the necessary back pressure to simulate the pressure conditions in the combustion chamber at the time of injection. This equipment is based on the Bosch method for the metering procedure, which consists of injecting the fuel into a measurement tube filled with the same fuel. A dynamic pressure wave is generated by the injection event, this being proportional in shape and amplitude to the RoI.[37,38]

The RoI measurement system has integrated equipment necessary for the control and acquisition of data, which are necessary for the calculation of the injection rate. The injected mass is recorded using a Mettler PM4800 DeltaRange precision balance with a precision of ±0.01 g. A Yokogawa DL708E oscilloscope is responsible for acquiring the energizing pulses measured by a clamp meter, the dynamic pressure wave, the pressure in the common-rail, and the back pressure of the system. A NI-6009 instrument is responsible for acquiring the pressure and temperature values of the fuel before and after the common-rail. Subsequently, all of these data will be processed by software developed to calculate the RoI.

2.4. Nozzle Discharge Coefficient from RoI Measures. With the RoI measures, it is possible to obtain the hydraulic characterization of the nozzles tested with the different fuels and at different injection pressures, that is, the discharge coefficient (C_d). The discharge coefficient is calculated using the following expression[32]

$$C_d = \frac{\dot{m}_f}{\dot{m}_{th}} = \frac{\dot{m}_f}{A\sqrt{2\rho_f(P_{rail} - P_{back})}} \quad (1)$$

where $\dot{m}_f$ is the measured RoI, $\dot{m}_{th}$ is the theoretical RoI, A is the exit area of the nozzle, ρ_f is the average density of the fluid in the nozzle geometry, P_{rail} is the injection pressure and P_{back} is the back pressure. The discharge coefficient for the different conditions can be represented in terms of Reynolds Number (Re), defined as[32]

$$Re = \frac{D_o}{\nu_f}\sqrt{\frac{2(P_{rail} - P_{back})}{\rho_f}} \quad (2)$$

where D_o is the geometric diameter of the nozzle outlet and ν_f is the kinematic viscosity of the fluid.

2.5. MF from RoI Estimation Procedure. As indicated previously, this work aims to validate a method to estimate the MF of different fuels when only the RoI is available, and there is no experimental facility available.

The MF and RoI can be obtained respectively from[22]

$$\dot{M}_f = A_f\rho_f u_f^2 \quad (3)$$

$$\dot{m}_f = A_f\rho_f u_f \quad (4)$$

where $\dot{M}_f$ is the measured MF, A_f is the effective area of the nozzle outlet, ρ_f is the average density of the fluid in the nozzle geometry, u_f is the effective velocity of the flow at the nozzle exit and $\dot{m}_f$ is the measured RoI.

The experimental measurements of MF used in the present work, and which were used to validate the procedure here proposed, were obtained with equipment whose scheme is similar to that presented in Figure 2.

https://doi.org/10.1021/acsomega.3c06917
ACS Omega XXXX, XXX, XXX−XXX

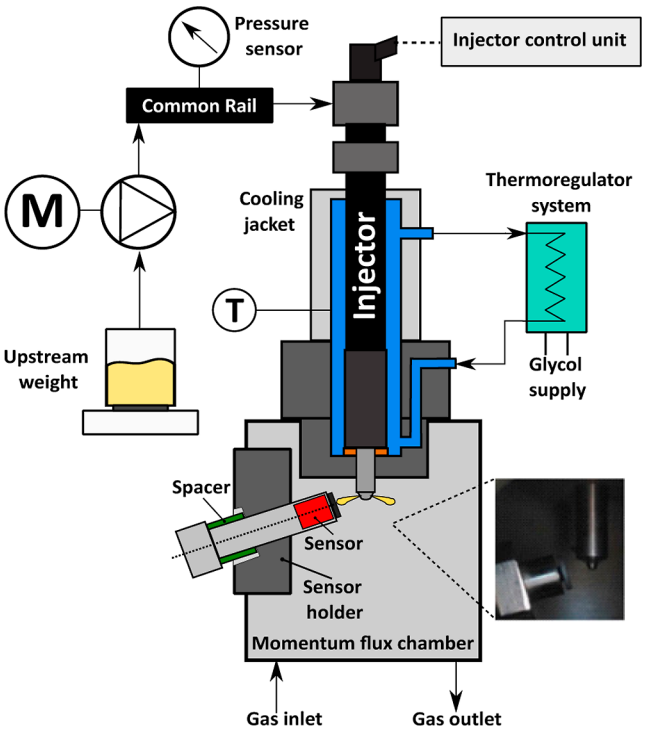

Figure 2. Scheme of the experimental facility used to measure MF.

Combining eqs 3 and 4, the MF and the RoI can be related with the following expression

$$\dot{M}_f = \frac{\dot{m}_f^2}{A_f \rho_f} \tag{5}$$

It is necessary to know A_f in order to obtain $\dot{M}_f$, so eq 1 is used and the following relation is obtained

$$C_d = \frac{\dot{m}_f}{\dot{m}_{th}} = \frac{A_f\sqrt{2\rho_f(P_{rail} - P_{back})}}{A\sqrt{2\rho_f(P_{rail} - P_{back})}} = \frac{A_f}{A} \tag{6}$$

Solve A_f in eq 6 yields the following expression

$$A_f = C_d A \tag{7}$$

Substitute eqs 7 in 5 is obtained

$$\dot{M}_f = \frac{\dot{m}_f^2}{C_d A \rho_f} \tag{8}$$

If $\dot{m}_f$ is solved from 5, is obtained

$$\dot{m}_f = \sqrt{\dot{M}_f A_f \rho_f} \tag{9}$$

Payri et al.[32] validated a method using eq 9 to determine the RoI as a function of MF measurement for four different fuels (diesel, biodiesel, GtL and Farnesane). They used an injector with seven holes and measured the MF in each one of them, and in order to apply the method, they made an average of the MF of all the holes. They found that the calculated rate of the injection profile had a high similarity to the experimental rate of the injection profile. They concluded that the applied method provides a valid RoI and that the maximum error in the calculation of the injected mass was around 11%. Figure 3 shows MF (Figure 3a) and RoI (Figure 3b) measured experimentally and calculated with eqs 5 and 9 of the work done by Payri et al.[32] The test corresponds to diesel fuel at an injection pressure of 90 MPa, an energization time of 2.5 ms, a fuel temperature of 313 K and a back pressure of 6 MPa.

This error may be due to intrinsic differences between the RoI rate measurement procedure and the MF procedure: the MF is measured in only one hole at a time, while the RoI considers all holes. In MF measurements, the injections are made in a gaseous medium, while in RoI measurements they are made in a liquid. The latter can cause the dynamics of the needle to change and lead to variations in the amount of injection and its distribution. To this, it must be added that the position of the measurement sensors of both procedures is located at different distances.

Therefore, for this work, eq 8 will be applied to determine the MF from the RoI measure. But an injector with a single hole will be used to avoid the measurement and calculation uncertainty that is obtained with injectors with more than one hole.

2.6. Data Processing. Figure 4 shows the graphs obtained after processing the data. In Figure 4a is the graph of the RoI, where the area marked in red is the one used to calculate the total mass injected. The Figure 4c,d correspond to the injection pressure and the back pressure, respectively. Finally, Figure 4b corresponds to the injector energization pulse.

Five repetitions were performed for each test. Therefore, to present the results, an average of all injection events was made. Figure 5 shows a test with all repetitions and the average. As can be seen in the graph, although the total number of repetitions for each operating condition is low, the cloud of points is quite

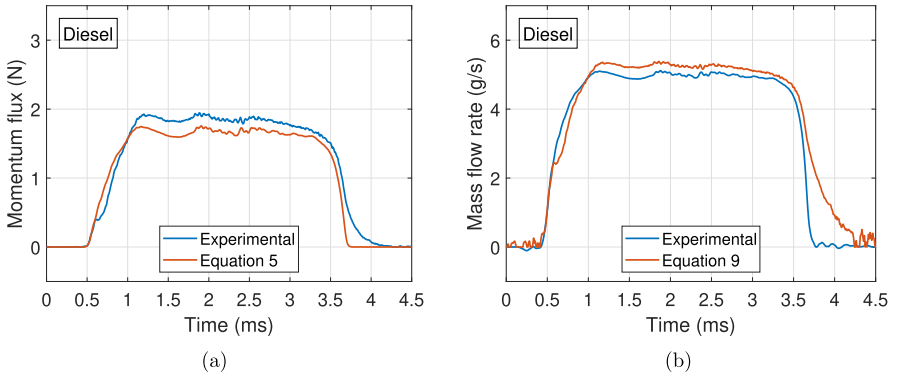

Figure 3. MF and fuel mass flow rate experimental data compared to results obtained by means of eqs 5 and 9 respectively. The Figure 3a corresponds to the MF, and the Figure 3b corresponds to the mass flow rate.

https://doi.org/10.1021/acsomega.3c06917
ACS Omega XXXX, XXX, XXX−XXX

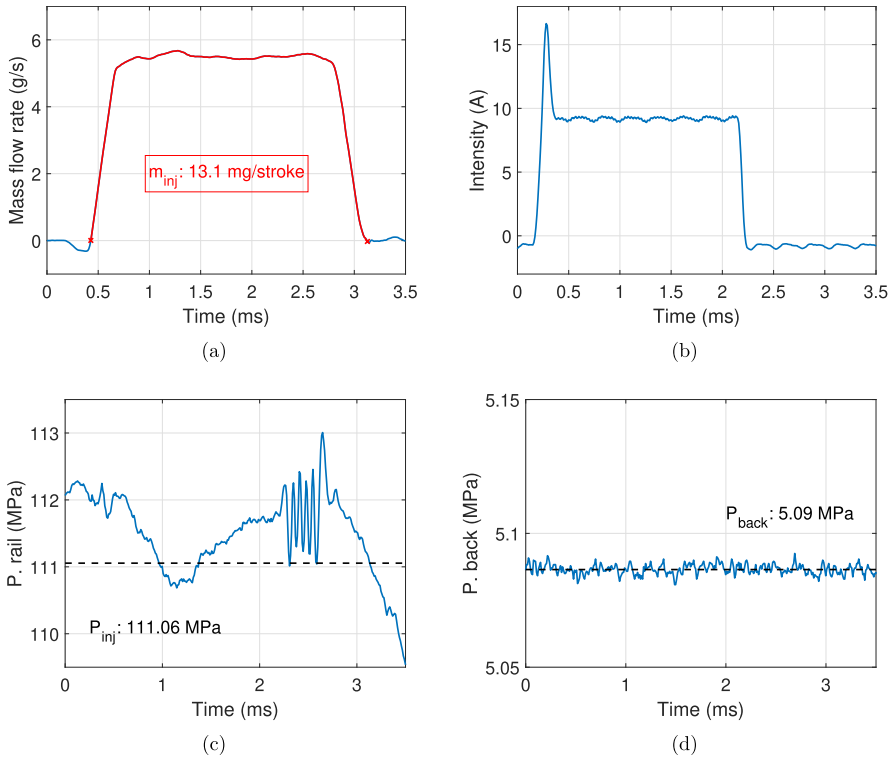

Figure 4. Graphics after processing. Nozzle: 150 μm. GtL fuel. P_{inj}: 110 MPa. ET: 2 ms. The (a) corresponds to the mass flow rate, the (b) corresponds to the injector energization pulse, the (c) corresponds to the injection pressure, and the (d) corresponds to the back pressure.

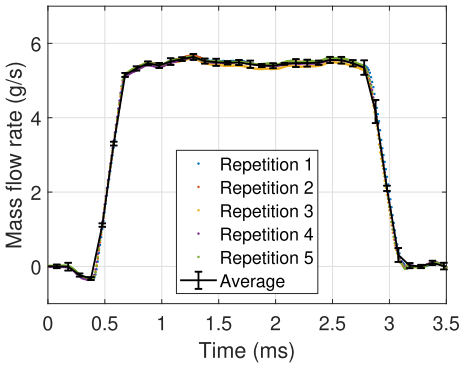

Figure 5. Mass flow rate cycle-to-cycle dispersion and averaged curve. Nozzle: 150 μm. GtL fuel. P_{inj}: 110 MPa. ET: 2 ms.

concentrated around the average curve, and the standard deviation is less than 15%. The deviation shown in the figure was similar to other test conditions at different pressure levels for all the tested fuels. Therefore, the use of the average curve for the representation of the results can be considered accurate.

3. RESULTS AND DISCUSSION

This section is divided into three parts. At first it presents the measured RoI using the Bosch method to verify the hydraulic behavior of the three tested nozzles and understand the effect of the fuel type. Later, the nozzle discharge coefficient calculation is presented. This is an important parameter for the subsequent estimation of the MF. In the last part, the MF is estimated from the RoI curves, following the procedure presented in eq 8.

3.1. RoI Results. Figure 6 shows a comparison of the measured RoI between fuels for the three nozzles, two injection pressures (90 and 110 MPa) and one energizing time (2 ms).

The curves of the RoI, presented in Figure 6, show the increase in the fuel mass flow rate proportionally to the square root of the difference between the common rail injection pressure and the back pressure of the fuel rate indicator. These results also show a decrease of the fuel mass flow rate, proportionally to the fuels density value, where the GtL fuel delivers lower mass amount compared to HVO fuel. This trend is in agreement with previous studies available in the literature that showed that the density is one of the main properties that influences the amount of mass injected.

3.2. Nozzle Discharge Coefficient Determination. Once the RoI measurements of all of the tests were obtained, they were used to calculate the discharge coefficient of the tested nozzles. Figure 7 shows the C_d values as a function of the Reynolds number for each of the nozzles. As can be seen, C_d has an asymptotic trend as a function of the Reynolds number. This indicates that the nozzle flow is fully developed. The value of the discharge coefficient depends on the characteristics of the injection system, particularly the geometry of the nozzle.[29,39] Besides, it is found that GtL fuel has a higher Reynolds number for the three nozzles compared with diesel and HVO fuels. This behavior was expected since the viscosity of GtL fuel is lower than the viscosity of diesel and HVO fuels. These last two have similar viscosity values.

As can be seen, the discharge coefficient values are different for the three tested nozzles. The smaller orifice nozzle has the largest discharge coefficient (closer to unity), meaning a more efficient discharge geometry. This is because these nozzles are conical, with the last one showing the larger half an gle. The coherence of the obtained values can be theoretically checked as follows below.

Equation 1 indicates the discharge coefficient definition. From this equation, the total available pressure can be expressed as

https://doi.org/10.1021/acsomega.3c06917
ACS Omega XXXX, XXX, XXX−XXX

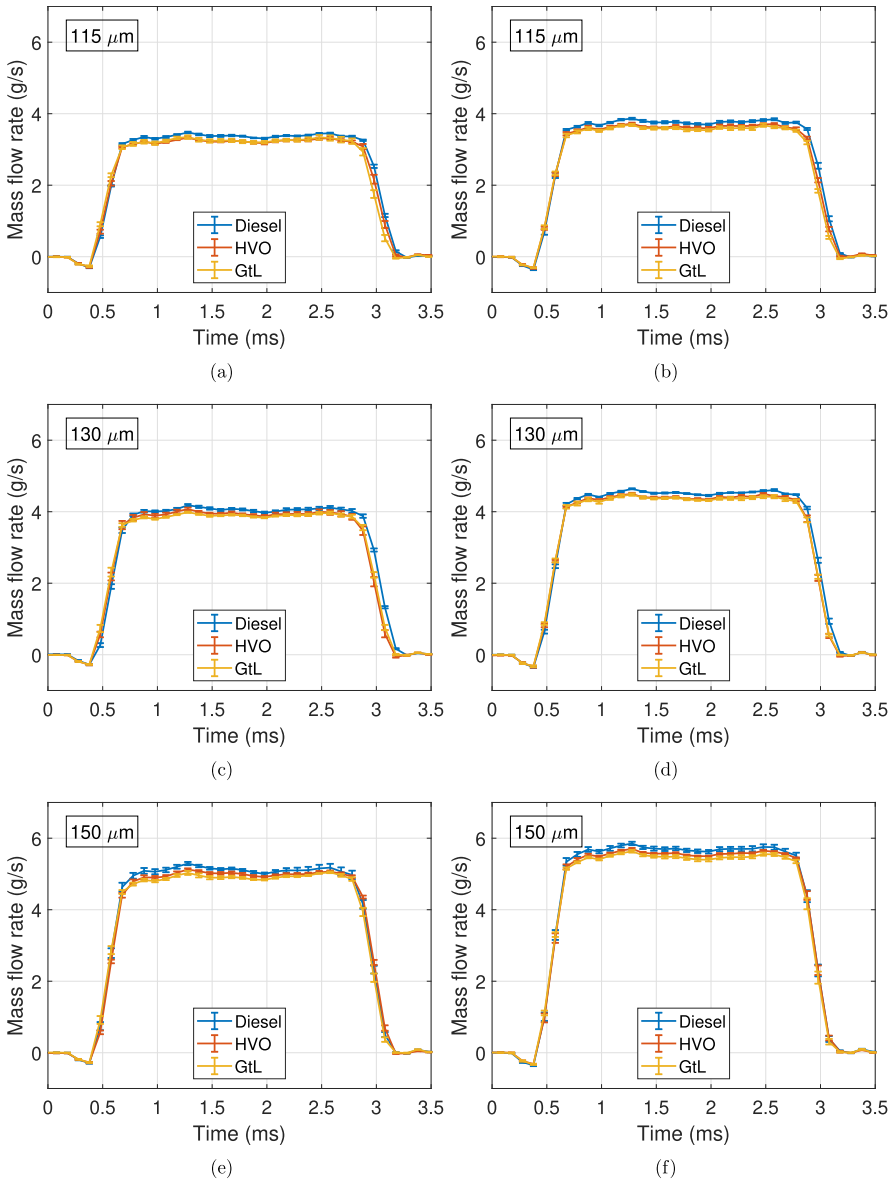

Figure 6. Comparison of the rates of injection between fuels. The Figures 10a,c,e correspond to a P_{inj}: 90 MPa, while the Figures 10b,d,f correspond to a P_{inj}: 110 MPa.

$$P_{rail} - P_{back} = \frac{1}{C_d^2}\frac{\dot{m}_f^2}{2A^2\rho_f} = \frac{1}{C_d^2}\frac{1}{2}\rho_f u_b^2 \tag{10}$$

where u_b is the bulk velocity associated with the mass-flow at the nozzle orifice. On the other hand, the relevant head losses in this kind of nozzle are (i) the outlet momentum, (ii) the friction along the nozzle duct, and (iii) the losses at the inlet. These are usually modeled as eq 11 indicates

$$p_{rail} - p_{back}\frac{1}{2}\rho_f u_b^2 + \frac{1}{2}\rho_f u_{b,average}^2 f\left(\frac{L}{D}\right)_{average} + \frac{1}{2}\rho_f u_{bi}^2 K_i \tag{11}$$

where f is the friction factor of the moody diagram, L is the nozzle length, D is the nozzle diameter and K_i is the inlet loss of head coefficient. Writing all the terms as a function of the outlet bulk velocity, and the inlet and outlet diameters the expression reads

$$p_{rail} - p_{back} = \frac{1}{2}\rho_f u_b^2 + \frac{1}{2}\rho_f u_b^2 f\frac{L}{D_o}\left(\frac{D_o(D_o + D_i(D_0^2 + D_i^2))}{D_i^4}\right) + \frac{1}{2}\rho_f u_b^2 K_i\left(\frac{D_o^4}{D_i^4}\right) \tag{12}$$

where D_i is the geometric diameter of the nozzle inlet. Direct comparison with eq 10, leads to

$$\frac{1}{C_d^2} = 1 + f\frac{L}{D_o}\left(\frac{D_o(D_o + D_i)(D_o^2 + D_i^2)}{D_i^4}\right) + K_i\left(\frac{D_o^4}{D_i^4}\right) \tag{13}$$

This means

$$C_d = \frac{1}{\sqrt{1 + f\frac{L}{D_o}\left(\frac{D_o(D_o + D_i)(D_o^2 + D_i^2)}{D_i^4}\right) + K_i\left(\frac{D_o^4}{D_i^4}\right)}} \tag{14}$$

https://doi.org/10.1021/acsomega.3c06917
ACS Omega XXXX, XXX, XXX−XXX

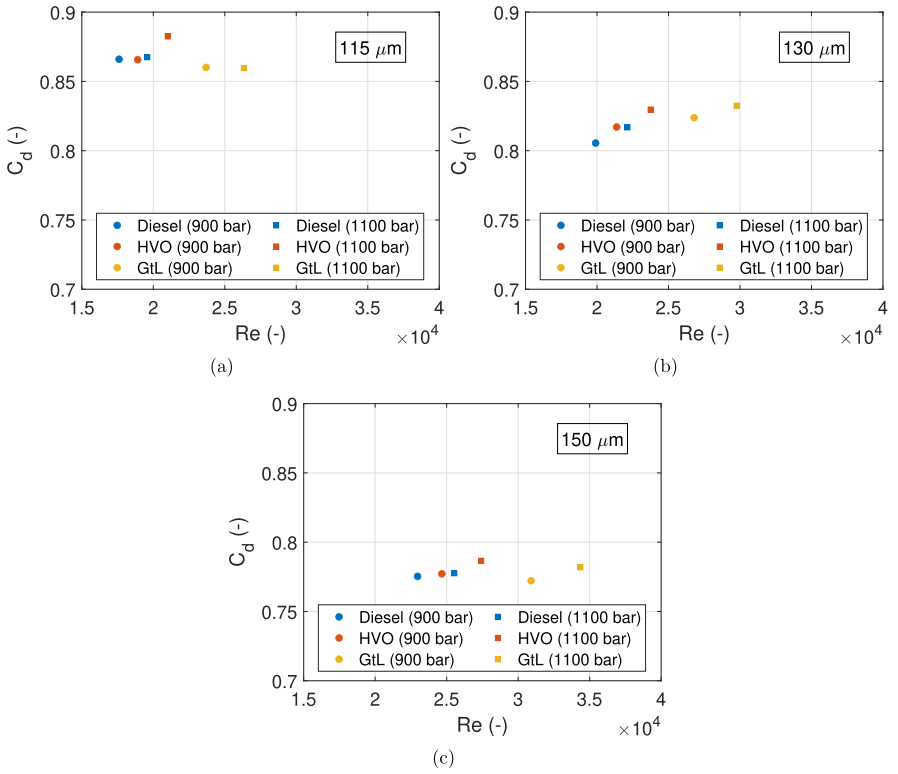

Figure 7. Discharge coefficients for all fuels and injection pressures. The (a) corresponds to the discharge coefficient of the nozzle of 115 μm, the (b) corresponds to the discharge coefficient of the nozzle of 130 μm and the (c) corresponds to the discharge coefficient of the nozzle of 150 μm.

Considering, as a first approximation, the usual value of K_i = 0.5, for the sharp-inlet loss of head, and an average value of f = 0.065, consistent with the Reynolds number based on the bulk velocity. Figure 8 shows the values of this theoretical approximation versus the measured ones.

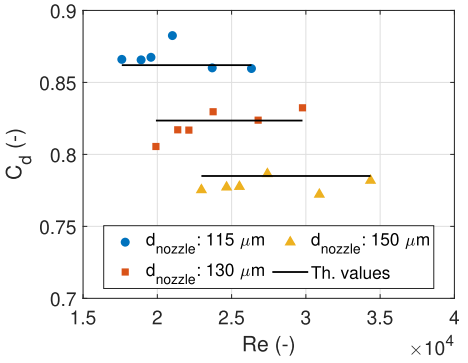

Figure 8. Discharge coefficient theoretical values versus measured values for the three tested nozzles. Depicted Reynolds number, Re, corresponds to eq 2. This Re is related to bulk velocity Reynolds as $Re_u b = ReC_d$.

3.3. Validation of the Procedure for the MF Estimation.

Figure 9 shows the validation of the method using eq 8. The data presented in Figure 3 were used to validate the method. The figure depicts three curves: the blue curve is the RoI measured directly with the Bosch apparatus, the orange curve represents the experimental MF, that is also used for validation, and the purple curve corresponds to the calculated one. It is observed that the MF calculated using eq 8 and the one measured experimentally showed good agreement. Therefore,

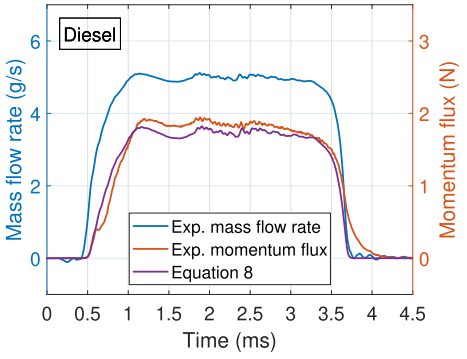

Figure 9. Validation of the method was carried out using eq 8.

the application of the method proposed in this work for the determination of the MF can be considered accurate.

In general, the MF determined from the RoI curve and eq 8 replicated the start of injection, the wave fluctuation in the stabilized phase, and the initial part of the closing stage. However, some characteristics can be identified:

- Opening phase: the start of injection can be well characterized. Usually there is a small difference in the initial stage of the injection process since the RoI is measured injecting into liquid, and the experimental spray MF for validation was obtained injecting into inert gas. Additionally, the transducers of both experimental approaches are located at different positions. In the momentum test rig the fuel spray has to travel some distance. Then, it takes a while for the first droplets going through the control volume and impact the force sensor downstream. To correct this phenomena, the signals were

https://doi.org/10.1021/acsomega.3c06917
ACS Omega XXXX, XXX, XXX−XXX

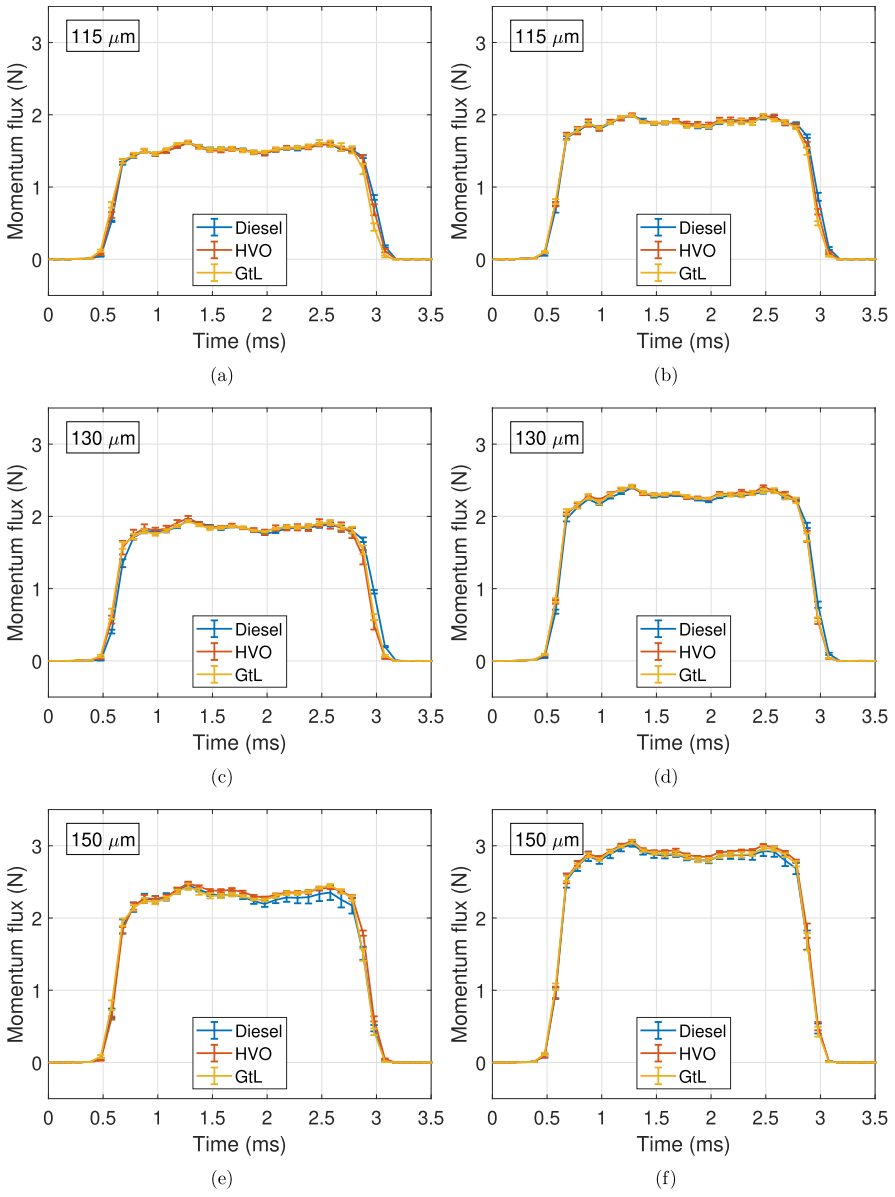

Figure 10. Comparison of the MF between fuels. The (a,c,e) correspond to a P_{inj}: 90 MPa, while the (b,d,f) correspond to a P_{inj}: 110 MPa.

phased with the RoI data considering the distance between the nozzle and the sensor, and the spray velocity.

Furthermore, the first part of the opening phase in the experimental spray momentum signal has two slopes that are not captured using the Bosch method. This can be attributed to the formation of packages of liquid that leave the nozzle at the beginning, where the dynamics of the needle is relevant. It is reflected then on the different velocities of the droplets at the spray tip when they impact at the force transducer.[40,41]

- Steady phase: in this study, the energizing time selected for the measurements are long enough to ensure that the needle of the injector is completely open and does not perturb the flow through the orifice. It can be seen that the MF obtained with eq 8, reproduces quite well this phase of the injection event, and the fluctuations due to the wave dynamics in the injector body and high pressure line are well captured.
- Closing phase: although the experimental and calculated curves have the same slope at the beginning of the injector closing, in the final phase the experimental curve has a much slower slope. This behavior is due to the fact that the injection has already finished, but the last drops of fuel slow down their movement and reach the transducer with less force. In this case, it could be considered that the curve obtained from the mass flow rate measurement best reproduces the end of the injection event.

Once the method has been validated with experimental, it will be used to estimate the MF for the three nozzle geometries and for the three fuels analyzed in this study.

3.4. MF Determination from RoI Measurements for Different Fuels. The experimental results obtained for the measured RoI together with eq 8 were used to determine the instantaneous MF. Figure 10 shows a comparison of the MF between fuels for the three nozzle diameters, two injection pressures (90 and 110 MPa) and one energizing time (2 ms).

These results indicate that for the range of injection pressures tested (typical of the operation of reciprocating ICEs) and for the studied injection nozzle diameter values (typical of current

https://doi.org/10.1021/acsomega.3c06917
ACS Omega XXXX, XXX, XXX−XXX

injection systems), the effect of HVO and GtL paraffinic fuels on the spray MF is similar to that produced by conventional diesel fuel. This result is interesting when introducing the use of these emerging alternate fuels in current engines. If these fuels have a similar behavior, from the point of view of the spray MF, it is expected that the lift off and the air entrainment during its introduction into the combustion chamber will also be similar, and consequently, the physical process of the air-fuel mixture formation before the start of combustion would be analogous.

4. CONCLUSIONS

A method for the determination of the spray MF was validated for three different fuels through the measurement of the RoI. The fuels tested were diesel, GtL and HVO. All test conditions were determined according to the most representative values of the real engine conditions. The main conclusions obtained in this work are:

A simple and reliable method is proposed for the estimation of the spray MF from the measurement of the RoI.

The proposed method of MF estimation has been compared with experimental measurements with good accuracy.

The proposed method has been applied to estimate the spray MF using two different sustainable and renewable fuels, such as a HVO and a GtL.

The differences in both density and viscosity between fossil diesel fuel and renewable HVO and GtL fuels are not significant enough to modify the spray MF under typical operation conditions with nozzles tested. This result is very welcome because it will contribute to an easier introduction of these fuels in current engines.

Based on the aforementioned results and conclusions, it is possible to state that the MF estimation method is realistic and accurate enough when only experimental equipment to measure the injection rate is available.

Summarizing, it can be said that the presented method provides an accurate spray MF curve despite being obtained from the RoI signal and the corresponding equations derived from the theory. Therefore, this means that only with the available mass flow measurement can an adequate prognosis be obtained in the case of not having access to an experimental setup for direct measurement of the MF.

AUTHOR INFORMATION

Corresponding Author

Octavio Armas − *Universidad de Castilla-La Mancha, Campus de Excelencia Internacional en Energía y Medioambiente, Instituto de Investigación Aplicada a la Industria Aeronáutica, Toledo 45071, Spain;* orcid.org/0000-0002-3675-1522; Email: octavio.armas@uclm.es

Authors

Lis Corral-Gómez − *Universidad de Castilla-La Mancha, Campus de Excelencia Internacional en Energía y Medioambiente, Instituto de Investigación Aplicada a la Industria Aeronáutica, Toledo 45071, Spain*

José A. Soriano − *Universidad de Castilla-La Mancha, Campus de Excelencia Internacional en Energía y Medioambiente, Instituto de Investigación Aplicada a la Industria Aeronáutica, Toledo 45071, Spain*

José-Ignacio Nogueira − *Universidad de Castilla-La Mancha, Campus de Excelencia Internacional en Energía y Medioambiente, Instituto de Investigación Aplicada a la Industria Aeronáutica, Toledo 45071, Spain*

Gabriela Bracho − *Universitat Politècnica de València. Instituto CMT-Motores Térmicos, Valencia E-46022, Spain*

Complete contact information is available at: https://pubs.acs.org/10.1021/acsomega.3c06917

Notes

The authors declare no competing financial interest.

ACKNOWLEDGMENTS

The authors wish to express their gratitude for the financial support provided by the Castilla-La Mancha Government to the project, ASUAV ref. SBPLY/19/180501/000116.

NOMENCLATURE

A	exit area of the nozzle
A_f	effective area of the nozzle outlet
C_a	area coefficient
C_d	discharge coefficient
D	nozzle diameter
D_i	geometric diameter of the nozzle inlet
D_o	geometric diameter of the nozzle outlet
f	friction factor of the moody diagram
K_i	inlet loss of head coefficient
L	nozzle length
$\dot{M}_f$	measured momentum flux
$\dot{m}_f$	measured rate of injection
$\dot{m}_{th}$	theoretical rate of injection
ν_f	kinematic viscosity of the fluid
P_{back}	back pressure
P_{rail}	injection pressure
ρ_f	average density of the fluid in the nozzle geometry
u_b	bulk velocity associated with the mass-flow at the nozzle orifice
u_f	effective velocity of the flow at the nozzle exit

REFERENCES

(1) Thangaraja, J.; Kannan, C. Effect of exhaust gas recirculation on advanced diesel combustion and alternate fuels-A review. *Appl. Energy* **2016**, *180*, 169−184.

(2) Speirs, J.; McGlade, C.; Slade, R. Uncertainty in the availability of natural resources: Fossil fuels, critical metals and biomass. *Energy Pol.* **2015**, *87*, 654−664.

(3) Parravicini, M.; Barro, C.; Boulouchos, K. Experimental characterization of GTL, HVO, and OME based alternative fuels for diesel engines. *Fuel* **2021**, *292*, 120177.

(4) Bohl, T.; Smallbone, A.; Tian, G.; Roskilly, A. P. Particulate number and NO trade-off comparisons between HVO and mineral diesel in HD applications. *Fuel* **2018**, *215*, 90−101.

(5) Pastor, J. V.; García-Oliver, J. M.; Micó, C.; García-Carrero, A. A.; Gómez, A. Experimental study of the effect of hydrotreated vegetable oil and oxymethylene ethers on main spray and combustion characteristics under engine combustion network spray a conditions. *Appl. Sci.* **2020**, *10*, 5460.

(6) Erkkilä, K.; Nylund, N.-O.; Hulkkonen, T.; Tilli, A.; Mikkonen, S.; Saikkonen, P.; Mäkinen, R.; Amberla, A. *Emission Performance of Paraffinic HVO Diesel Fuel in Heavy Dduty Vehicles. SAE Technical paper*; SAE, 2011; Vol. *01*, p 1966.

(7) Aatola, H.; Larmi, M.; Sarjovaara, T.; Mikkonen, S. Hydrotreated vegetable oil (HVO) as a renewable diesel fuel: trade-off between NO_x, particulate emission, and fuel consumption of a heavy duty engine. *SAE Int. J. Engines* **2008**, *1*, 1251−1262.

(8) Ram, V.; Salkuti, S. R. An Overview of Major Synthetic Fuels. *Energies* **2023**, *16*, 2834.

https://doi.org/10.1021/acsomega.3c06917
ACS Omega XXXX, XXX, XXX−XXX

(9) da Costa, R. B. R.; Roque, L.; de Souza, T.; Coronado, C.; Pinto, G.; Cintra, A.; Raats, O.; Oliveira, B.; Frez, G.; da Silva, M. Experimental assessment of renewable diesel fuels (HVO/Farnesane) and bioethanol on dual-fuel mode. *Energy Convers. Manage.* **2022**, *258*, 115554.
(10) Abu-Jrai, A.; Tsolakis, A.; Theinnoi, K.; Cracknell, R.; Megaritis, A.; Wyszynski, M.; Golunski, S. Effect of gas-to-liquid diesel fuels on combustion characteristics, engine emissions, and exhaust gas fuel reforming. Comparative study. *Energy Fuels* **2006**, *20*, 2377−2384.
(11) Krahl, J.; Knothe, G.; Munack, A.; Ruschel, Y.; Schröder, O.; Hallier, E.; Westphal, G.; Bünger, J. Comparison of exhaust emissions and their mutagenicity from the combustion of biodiesel, vegetable oil, gas-to-liquid and petrodiesel fuels. *Fuel* **2009**, *88*, 1064−1069.
(12) Kitano, K.; Misawa, S.; Mori, M.; Sakata, I.; Clark, R. H. GTL Fuel Impact on Dl Diesel Emissions. *SAE Trans.* **2007**, *116*, 603−611.
(13) Kitano, K.; Sakata, I.; Clark, R. Effects of GTL fuel properties on DI diesel combustion. *SAE Trans.* **2005**, *114*, 1415−1425.
(14) Hürpekli, M.; Necati Özsezen, A. Determination of combustion and emission characteristics of liquid Fischer−Tropsch diesel fuel synthesized from coal in a diesel engine. *Energy Convers. Manage.* **2023**, *292*, 117351.
(15) Fayad, M. A.; Tsolakis, A.; Martos, F. J. Influence of alternative fuels on combustion and characteristics of particulate matter morphology in a compression ignition diesel engine. *Renewable Energy* **2020**, *149*, 962−969.
(16) Emiroğlu, A. O. Effect of fuel injection pressure on the characteristics of single cylinder diesel engine powered by butanol-diesel blend. *Fuel* **2019**, *256*, 115928.
(17) Agarwal, A. K.; Dhar, A.; Gupta, J. G.; Kim, W. I.; Choi, K.; Lee, C. S.; Park, S. Effect of fuel injection pressure and injection timing of Karanja biodiesel blends on fuel spray, engine performance, emissions and combustion characteristics. *Energy Convers. Manage.* **2015**, *91*, 302−314.
(18) Anggono, W.; Ikoma, W.; Chen, H.; Liu, Z.; Ichiyanagi, M.; Suzuki, T.; Gotama, G. J. Investigation of intake pressure and fuel injection timing effect on performance characteristics of diesel engine. *IOP Conf. Ser. Earth Environ. Sci.* **2019**, *257*, 012037.
(19) Agarwal, A. K.; Chaudhury, V. H. Spray characteristics of biodiesel/blends in a high pressure constant volume spray chamber. *Exp. Therm. Fluid Sci.* **2012**, *42*, 212−218.
(20) Mata, C.; Piaszyk, J.; Soriano, J. A.; Herreros, J. M.; Tsolakis, A.; Dearn, K. Impact of alternative paraffinic fuels on the durability of a modern common rail injection system. *Energies* **2020**, *13*, 4166.
(21) Mohan, B.; Yang, W.; Tay, K. L.; Yu, W. Macroscopic spray characterization under high ambient density conditions. *Exp. Therm. Fluid Sci.* **2014**, *59*, 109−117.
(22) Payri, R.; Garcia, J.; Salvador, F.; Gimeno, J. Using spray momentum flux measurements to understand the influence of diesel nozzle geometry on spray characteristics. *Fuel* **2005**, *84*, 551−561.
(23) Rajaratnam, N. *Turbulent jets*; Elsevier, 1976.
(24) Payri, R.; Ruiz, S.; Salvador, F.; Gimeno, J. On the dependence of spray momentum flux in spray penetration: Momentum flux packets penetration model. *J. Mech. Sci. Technol.* **2007**, *21*, 1100−1111.
(25) Corral-Gómez, L.; Castillo-García, F. J.; Soriano, J. A.; Armas, O. Macroscopic Parameters of Fuel Sprays Injected in an Optical Reciprocating Single-Cylinder Engine: An Approximation by Means of Visualization with Schlieren Technique. *Sensors* **2023**, *23*, 6747.
(26) Corral-Gómez, L.; Martos, F. J.; Fernández-Yáñez, P.; Armas, O. A CFD Modelling Approach of Fuel Spray under Initial Non-Reactive Conditions in an Optical Engine. *Energies* **2023**, *16*, 6537.
(27) Corral-Gómez, L.; Armas, O.; Soriano, J. A.; Pastor, J. V.; García-Oliver, J. M.; Micó, C. An Optical Engine Used as a Physical Model for Studies of the Combustion Process Applying a Two-Color Pyrometry Technique. *Energies* **2022**, *15*, 4717.
(28) Desantes, J. M.; Payri, R.; Salvador, F. J.; Gil, A. Development and validation of a theoretical model for diesel spray penetration. *Fuel* **2006**, *85*, 910−917.
(29) Desantes, J.; Payri, R.; Garcia, J.; Salvador, F. A contribution to the understanding of isothermal diesel spray dynamics. *Fuel* **2007**, *86*, 1093−1101.
(30) Martos, F. J.; Soriano, J. A.; Mata, C.; Armas, O.; Soto, F. Impact of alternative and fossil diesel fuels on internal flow of injection nozzle. *Int. J. Engine Res.* **2022**, *23*, 940−957.
(31) Payri, R.; Salvador, F.; Gimeno, J.; Bracho, G. A new methodology for correcting the signal cumulative phenomenon on injection rate measurements. *Exp. Tech.* **2008**, *32*, 46−49.
(32) Payri, R.; Bracho, G.; Soriano, J. A.; Fernández-Yáñez, P.; Armas, O. Nozzle rate of injection estimation from hole to hole momentum flux data with different fossil and renewable fuels. *Fuel* **2020**, *279*, 118404.
(33) Desantes, J.; Payri, R.; Salvador, F.; Gimeno, J. *Measurements of Spray Momentum for the Study of Cavitation in Diesel Injection Nozzles. SAE Paper*; SAE, 2003; Vol. *01*, p 0703.
(34) He, Z.; Shao, Z.; Wang, Q.; Zhong, W.; Tao, X. Experimental study of cavitating flow inside vertical multi-hole nozzles with different length−diameter ratios using diesel and biodiesel. *Exp. Therm. Fluid Sci.* **2015**, *60*, 252−262.
(35) Mata, C.; Rojas-Reinoso, V.; Soriano, J. A. Experimental determination and modelling of fuel rate of injection: A review. *Fuel* **2023**, *343*, 127895.
(36) Armas, O.; Martínez-Martínez, S.; Mata, C.; Pacheco, C. Alternative method for bulk modulus estimation of Diesel fuels. *Fuel* **2016**, *167*, 199−207.
(37) Bosch, W. The fuel rate indicator: a new measuring instrument for display of the characteristics of individual injection. *SAE Trans.* **1967**, *75*, 641−662.
(38) Komaroff, I.; Melcher, K. *The Fuel Quantity Indicator-A New Measuring Device for Voltric Evaluation of Individual Fuel Injection Quantities. SAE Technical Paper*; SAE, 1966.
(39) Lichtarowicz, A.; Duggins, R. K.; Markland, E. Discharge coefficients for incompressible non-cavitating flow through long orifices. *J. Mech. Eng. Sci.* **1965**, *7*, 210−219.
(40) Desantes, J.; Payri, R.; Salvador, F.; Gimeno, J. *Prediction of Spray Penetration by Means of Spray Momentum Flux. SAE paper*; SAE, 2006; Vol. *01*, p 1387.
(41) Postrioti, L.; Mariani, F.; Battistoni, M. Experimental and numerical momentum flux evaluation of high pressure Diesel spray. *Fuel* **2012**, *98*, 149−163.

https://doi.org/10.1021/acsomega.3c06917
ACS Omega XXXX, XXX, XXX−XXX